Ab initio structure determination of the hygroscopic anhydrous form of α-lactose by powder X-ray diffraction

Cyril Platteau, Jacques Lefebvre,* Frederic Affouard and Patrick Derollez

Laboratoire de Dynamique et Structure des Matériaux Moléculaires (UMR CNRS 8024), UFR de Physique, Bâtiment P5, Université des Sciences et Technologies de Lille, 59655 Villeneuve d'Ascq Cédex, France

Correspondence e-mail:
jacques.lefebvre@univ-lille1.fr

Annealing of α-lactose monohydrate at 408 K yielded a mixture of this compound with hygroscopic anhydrous α-lactose. A powder X-ray diffraction pattern of this mixture was recorded at room temperature. The starting structural model of hygroscopic α-lactose was found by a Monte Carlo simulated-annealing method. The final structure was obtained through Rietveld refinements, with soft restraints on interatomic bond lengths and bond angles, and crystalline energy minimization to locate the H atoms of the hydroxy groups. The crystalline cohesion is achieved by networks of $O-H\cdots O$ hydrogen bonds that differ from those of the monohydrate phase. The width of the Bragg peaks is interpreted by a phenomenological microstructural approach in terms of isotropic size effects and anisotropic strain effects.

1. Introduction

Lactose (4-*O*-β-D-galactopyranosyl-D-glucopyranose), also called milk sugar, is a carbohydrate comprising one galactose moiety linked to a glucose molecule through a β-1,4 linkage. Lactose exhibits two anomeric forms, α-lactose and β-lactose, which differ in the configuration of the terminal hydroxy group of the glucose unit for the β-form; the atoms O1′ and H1′ of Fig. 2 are inverted. In the solid state, lactose can be amorphous or crystallized, and five crystalline forms are known (Garnier, 2001): α-lactose monohydrate (hereafter named $\alpha L-H_2O$), hygroscopic anhydrous α-lactose (αL_H), stable anhydrous α-lactose (αL_S), β-lactose (βL) and mixed compounds, α/β, with different stoichiometries ($\alpha/\beta L$). The crystalline structures have been solved for only two of these five forms: they are $\alpha L-H_2O$ (Fries *et al.*, 1971; Beevers & Hansen, 1971; Noordik *et al.*, 1984) and βL (Hirotsu & Shimada, 1974). These are the only two forms that are commercially available and that give single crystals of adequate size for a single-crystal structure determination.

The αL_H phase was observed for the first time by Buma & Wiegers (1967). It is obtained by heat-drying the $\alpha L-H_2O$ form at ∼403 K. This form is unstable because it returns to the $\alpha L-H_2O$ form when the temperature is lowered and, upon heating, the αL_S phase appears (van Kreveld, 1969). It is therefore impossible to grow single crystals suitable for X-ray automatic diffractometer experiments; only powder diffraction patterns can be used for the crystalline structure determination of the αL_H phase.

The aim of this paper is the structure determination of the αL_H form from powder X-ray diffraction experiments using the Rietveld method. In order to locate the H atoms of the hydroxy groups involved in hydrogen bonds, Rietveld refinements are complemented by energy minimization.

research papers

2. Experimental

2.1. Procedure to obtain the αL_H phase

Commercially available αL-H_2O was used for this experiment (Sigma). It is well known that this compound always contains a component of βL (Noordik et al., 1984; 4% for αL-H_2O from Sigma). A preliminary X-ray powder diffraction pattern of this compound does not exhibit Bragg peaks corresponding to the βL phase; there is no βL crystallite, but βL molecules can substitute for αL molecules in the monohydrate.

In order to obtain the αL_H phase, the following procedure was used: αL-H_2O powder contained in a crystallizer was annealed in an oven for 30 min at temperature T. To avoid possible rehydration, the powder was introduced into a Lindemann glass capillary and then sealed rapidly for the X-ray powder diffraction experiment. Attempts were performed at different temperatures. For temperatures lower than 393 K, only the peaks of the αL-H_2O phase were present in the patterns. From 398–408 K, in addition to the peaks of the αL-H_2O phase, new peaks appear, which correspond to the αL_H phase according to Buma & Wiegers (1967). At 413 K, the αL-H_2O form disappears and, as well as the peaks of the αL_H form, there are new diffraction peaks characterizing the αL_S phase (van Kreveld, 1969). Powder not used for the X-ray experiment was kept in air. After a week, this powder was analysed by X-ray diffraction and only the αL-H_2O phase was found. This experiment confirms that the supplementary peaks correspond to the unstable hygroscopic αL_H phase.

In conclusion, the αL_H form is always present with the αL-H_2O phase. Consequently, the pattern recorded at 408 K was chosen for structure determination, because this pattern has the best ratio of αL_H to αL-H_2O.

2.2. Data collection

The powder X-ray diffraction patterns were measured on a laboratory diffractometer equipped with an INEL curved, position-sensitive detector (CPS120). A bent quartz monochromator allowed selection of the $K\alpha_1$ wavelength of a Cu X-ray tube (λ = 1.54056 Å). The powder was introduced in a Lindemann glass capillary (diameter 0.7 mm) mounted on the axis of the diffractometer. The capillary was rotated during the experiment in order to reduce the effect of possible preferential orientations. Calibration of the curved detector was performed with an X-ray diffraction pattern of the standard compound $Na_2Ca_3Al_2F_{14}$ (NAC; Evain et al., 1993). A cubic spline interpolation was performed between the peaks of NAC. The curved detector has 4096 channels, the 2θ range recorded was 0.3–114.7° and the step between two channels was 0.029°. The pattern of NAC was also used to determine the shape and the parameters of the experimental resolution; it is a pseudo-Voigt function, with the Caglioti function for the θ dependence of the Gaussian component (Caglioti et al., 1958). The values of the parameters are U_{ins} = 0.0166 (4), V_{ins} = −0.0163 (4) and W_{ins} = 0.0101 (2) deg^2. The θ dependence of the Lorentzian component is such that

$$\Gamma_L = X_{ins} \tan\theta + Y_{ins}/\cos\theta,$$

with X_{ins} = 0.0076 (14) and Y_{ins} = 0.0197 (7)°. Data were collected at room temperature with a total counting time of 16 h 40 min.

2.3. Structure solution and refinement

For the determination of the lattice parameters of αL_H, the profiles of the 58 reflections with a 2θ angle lower than 40° were refined individually with the program WinPlotr (Roisnel & Rodriguez-Carvajal, 2002) in order to obtain their 2θ positions. The positions of the Bragg peaks of the αL-H_2O phase can be calculated from the lattice parameters obtained during structure determination (Fries et al., 1971). Among these 58 reflections, 14 of them, ranging from 9 to 33°, do not belong unambiguously to the αL-H_2O phase. The 2θ values of these reflections were input to the program TREOR (Werner et al., 1985) and these reflections were indexed completely, with a monoclinic cell, yielding the following parameters: a = 7.766, b = 19.698, c = 4.901 Å, β = 103.59° and V = 728.8 Å^3. The calculated figures of merit are $M(14)$ = 16 and $F(14)$ = 20 (0.017, 41) (de Wolff, 1968; Smith & Snyder, 1979). The volume found with TREOR is almost the same as that obtained for the cell of the βL phase (V = 716.7 Å^3; Hirotsu & Shimada, 1974) and that for β-cellobiose, which is a disaccharide with a β-1,4 linkage (V = 728.8 Å^3; Chu & Jeffrey, 1968). Therefore, the three cells have the same number of molecules (Z = 2).

The powder X-ray diffraction pattern from 8.5 to 62° 2θ was refined with the 'profile matching' option [Le Bail et al. (1988) profile refinement] of the program FullProf (Rodriguez-Carvajal, 2001). The refined angular range starts at 8.5°, in order to include the first reflection of the pattern at $\sim$9°; the upper limit was chosen to be 62°, since the intensities of the peaks become very low at higher angles. The monoclinic cell of Fries et al. (1971), with space group $P2_1$ for the αL-H_2O phase, and the previous cell for αL_H, with space group $P2$ (a space group without systematic extinction), were used in FullProf. The profile of the reflections was fitted with a pseudo-Voigt function with the same FWHM for the Gaussian and the Lorentzian components. This FWHM has a θ dependence according to the Caglioti law (Caglioti et al., 1958), and the Lorentzian contribution to the pseudo-Voigt function is a linear function of 2θ. The parameters to fit the profile of the reflections are different for the two phases. The asymmetry of the peaks was taken into account according to the Bérar & Baldinozzi (1993) function, with common parameters for the two phases. The background was determined with a linear interpolation between 26 points regularly distributed from 8.5 to 62°.

For αL_H, the systematic absence of $0k0$ reflections with k odd lead to the space group $P2_1$, and the asymmetric unit contains one molecule. At the end of the Le Bail refinements, the profile reliability factors are R_p = 0.0799, R_{wp} = 0.0850, R_{exp} = 0.0217 and χ^2 = 15.3; the lattice parameters of the αL_H phase are a = 7.7692 (5), b = 19.6971 (13), c = 4.9040 (4) Å, β = 103.731 (5)° and V = 729.0 (1) Å^3.

Table 1
Values of the bond lengths (Å) and bond angles (°) used for the soft restraints.

The index 'int' represents internal atoms of the cycles and 'per' the peripheral atoms; C and O atoms of the methanol groups are named C_m and O_m; O_{link} is the O atom linking the two units.

$C_{int}-C_{int}$	1.527
$C_{int}-O_{int}$	1.433
$C_{int}-C_m$	1.511
$C_{int}-O_{per}$, $C_{int}-O_{link}$, C_m-O_m	1.421
$C_{int}-C_{int}-C_{int}$	110.4
$C_{int}-C_{int}-O_{int}$	109.6
$C_{int}-O_{int}-C_{int}$	113.2
$C_{int}-C_{int}-C_m$	112.8
$O_{int}-C_{int}-C_m$	107.1
$C_{int}-C_{int}-O_{per}$	110.4
$C_{int}-C_m-O_m$	108.4
$O_{int}-C_{int}-O_{per}$	109.5
$C_{int}-C_{int}-O_{link}$, $O_{int}-C_{int}-O_{link}$	107.9
$C_{int}-O_{link}-C_{int}$	116.8

In order to obtain a starting structural model, the 'parallel tempering' algorithm of the program *FOX* (Favre-Nicolin & Cerny, 2002) was used. The 2θ angular range used in *FOX* was 8.5–50°. Lattice and profile parameters for the two phases, and the zero point and interpolated background calculated with the Le Bail refinements, were used in this program. For the αL-H_2O phase, the reduced coordinates of the C and O atoms found in the structure determination of Fries *et al.* (1971) were input to *FOX*, and these were refined in the following way. For the αL_H phase, a molecule of α-lactose, with C and O atoms only, was modelled with bond lengths, bond angles and torsion angles calculated from the atomic coordinates of Fries *et al.* (1971). This molecule was introduced randomly into the cell. During the calculation, all bond lengths and bond angles were kept constant, and the two central cycles of the galactose and glucose units were kept rigid. Torsion angles of the central linkage and those of peripheral O and C atoms were treated as free parameters, leading to 19 degrees of freedom: two translations (for space group $P2_1$, the translation along b must be restrained) and three rotations of the whole molecule, ten torsion angles for the peripheral atoms and four torsion angles for the central linkage. The temperature factors of the C and O atoms of the two phases could vary. The displacement parameters of the C and O atoms of the two phases were also refined freely. After about ten million trials, the R_w factor was 0.097, and no significant improvement of this factor was observed when more trials were carried out. The coordinates of non-H atoms found by *FOX* for the αL_H phase can be considered as a starting solution for the Rietveld refinements.

Parameters obtained from *FOX* were introduced into the program *FullProf*. It is well known that accurate determination of the positions of H atoms from powder X-ray diffraction experiments is impossible. In the present case, the positions of some of the H atoms can be deduced from geometrical arguments, as is the case for the H atoms of the CH and CH_2 groups. For H atoms of OH groups involved in hydrogen

bonds, an additional lattice energy minimization is needed as an aid to the X-ray experiments. The positions of the H atoms were calculated with the program *DEBVIN* (Brückner & Immirzi, 1997). For the CH groups, the H atoms were positioned such that the tetrahedron contained three equal C—C—H or O—C—H angles, with a C—H bond length of 1.00 Å. For the CH_2 groups, the H—C—H bond angle is 108°, the C—H bond length is 1.00 Å and the H/C/H plane is perpendicular to the C/C/O plane, the two H atoms being symmetrically located with respect to the C/C/O plane. Before energy calculations, and provisionally, the H atoms of hydroxy groups were positioned such that the C, O and H atoms are aligned. During the following refinements, this procedure was repeated several times in order to determine the correct positions of the H atoms.

The 2θ range for the Rietveld refinements was 8.5–80°. The reduced coordinates of the 23 non-H atoms were adjusted (the y coordinate of the central O atom was fixed at 0 and chosen as the origin). Owing to the large number of free parameters, soft restraints on all bond lengths and all bond angles were introduced. The values of these restraints were taken to be the mean values found in some disaccharides with a β-1,4 linkage (Chu & Jeffrey, 1968; Ham & Williams, 1970, Fries *et al.*, 1971; Hirotsu & Shimada, 1974). Table 1 gives these values for the different combinations of atoms involved in lactose. For the αL-H_2O phase, the input coordinates of the C, O and H atoms were those obtained by Fries *et al.* (1971); the molecule of lactose was taken to be a rigid body, which can translate and rotate around its mass centre. For each phase, all atoms were assigned a common isotropic displacement parameter. Intensities were corrected to the absorption effects for a cylindrical sample with a μR value of 0.40.

For the peak-shape function, a Thompson–Cox–Hastings profile function (Thompson *et al.*, 1987) was used, taking into account experimental resolution, and strain and size effects. The angular dependencies of the FWHM of the Gaussian (H_{Gf}) and Lorentzian (H_{Lf}) components of the peak profile are given by Rodriguez-Carvajal & Roisnel (2004).[1]

For the αL-H_2O phase, the less abundant form in the powder, the two effects were taken as isotropic. For the αL_H phase, among the four possibilities, the best choice, in terms of agreement factors, is when isotropic size effects and anisotropic strain effects are considered (for isotropic strains, R_{wp} = 0.0995, and it becomes equal to 0.0733 when they are taken as anisotropic). In this case, the Stephens (1999) formulation is
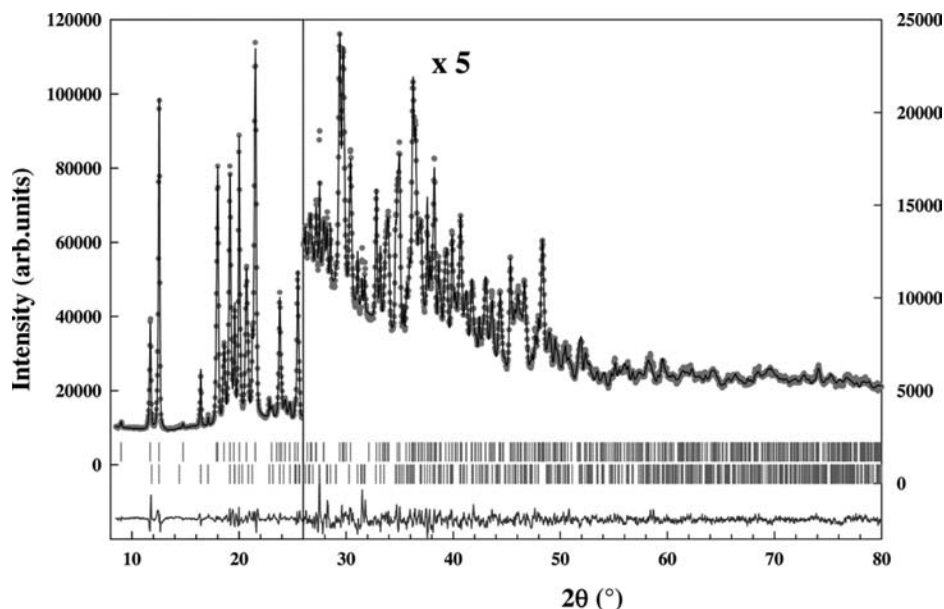
---

[1] The analytical expression of the Gaussian (H_{Gf}) and Lorentzian (H_{Lf}) components of the peak profile are

$$H_{Gf}^2 = [U_{ins} + U_{ST} + (1-\xi)^2 D_{ST}^2(a_{ST})]\tan^2\theta + V_{ins}\tan\theta + W_{ins} + G_{SZ}/\cos^2\theta$$

and

$$H_{Lf} = [X_{ins} + X_{ST} + \xi D_{ST}(a_{ST})]\tan\theta + [Y_{ins} + Y_{SZ} + F_{SZ}(S_{SZ})/\cos\theta],$$

where the subscript ST represents strain effects and SZ size effects.
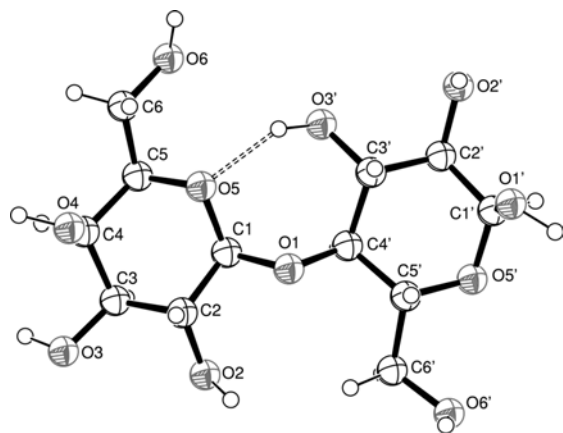
Figure 1
Final Rietveld plot. Observed data points are indicated by dots; the best-fit profile (upper trace) and the difference pattern (lower trace) are shown as solid lines. The vertical bars correspond to the positions of Bragg peaks (upper bars for αL_H, lower bars for αL-H_2O).

static interactions were handled by the Ewald method. We worked in the NVE statistical ensemble, where the number of atoms (N), the volume (V) and the energy (E) are fixed. A cut-off radius of 10 Å was used. In order to determine the positions of the hydroxy H atoms, energy minimization calculations ($T = 0$) were carried out from the structure obtained experimentally. The C—O—H angles were initially chosen to be 180°. No dihedral interaction is applied to the hydroxy H atoms. During minimization, only H atoms of the hydroxy groups are allowed to move, in order to maintain the experimental structure as much as possible.

In the final Rietveld refinements and for a 2θ range of 8.5–80°, there were 136 adjustable parameters:

(i) 18 profile parameters: the zero-point parameter, four lattice parameters, Y_{SZ}, G_{SZ}, nine parameters for the anisotropic strain effects and two parameters of the Bérar & Baldinozzi (1993) function for the asymmetry of the peaks.

used for $D_{ST}(a_{ST})$. X_{ST} and ξ are zero and the anisotropic strain effects only have Gaussian components.

The March (1932) and Dollase (1986) function was used to take into account the preferred orientations. After several trials, the best agreement factors were obtained for preferred orientations along [001] for αL_H and [010] for αL-H_2O.

Calculations were performed using the *DL_POLY* molecular modelling package (Smith & Forester, 1996) on a system of $N = 80$ ($4 \times 2 \times 5$ crystalline cells) lactose molecules using periodic boundary conditions. Each molecule is described by its 45 atoms, which interact through the Ha force-field (Ha *et al.*, 1988) developed for carbohydrates. Electro-

(ii) 71 structural parameters: the scale factor, 68 adjustable coordinates, a parameter (G_1) linked to preferred orientations [March (1932) and Dollase (1986) function] and a global isotropic displacement parameter. The number of adjustable parameters is, in fact, reduced by the introduction of 24 soft restraints on bond lengths and 35 on bond angles.

(iii) 15 parameters for the αL-H_2O phase: the scale factor, four lattice parameters, two degrees of translation and three degrees of rotation of the whole molecule of lactose, U_{ST}, Y_{SZ} and G_{SZ} for the profile of the peaks, G_1 for the preferred orientation function, and a global isotropic displacement parameter.

(iv) 32 points to define the background.

The final Rietveld agreement factors are $R_p = 0.0657$, $R_{wp} = 0.0733$, $R_{exp} = 0.0222$ and $\chi^2 = 10.9$. For the αL_H phase, $R_B = 0.0163$ and $R_F = 0.0223$; for the αL-H_2O phase, $R_B = 0.0468$ and $R_F = 0.0338$. The mean deviations from the soft restraints are 0.009 Å for the bond lengths and 4.4° for the bond angles. A plot of the X-ray pattern is given Fig. 1. The calculated specific percentage of the αL_H phase contained in the powder is 83 (1) %. A view of the molecule of lactose drawn with *ORTEP*-3 (Farrugia, 1997) and showing the atomic numbering scheme is presented in Fig. 2. Crystallographic data, and profile and structural parameters, are reported in Tables 2 and 3, respectively.[2]

Figure 2
Atomic numbering and molecular structure of the hygroscopic phase of α-lactose. The dashed lines represent the internal hydrogen bond of the molecule of lactose.

Table 2
Crystallographic data for the hygroscopic phase of α-lactose obtained after Rietveld refinements.

Formula	$C_{12}H_{22}O_{11}$
M_r	342.30
Crystal system	Monoclinic
Space group	$P2_1$
a (Å)	7.7795 (3)
b (Å)	19.6931 (7)
c (Å)	4.9064 (1)
β (°)	103.691 (2)
V (Å^3)	730.32 (4)
Z	2
D_c (Mg m^{-3})	1.557
$F(000)$	364
μ (mm^{-1})	1.22
2θ range (°)	8.5–80
Step size (° 2θ)	0.029
Wavelength (Å)	1.54056
No. of profile data steps	2465
No. of contributing reflections	1073
No. of structural variables	71
No. of profile parameters	18
No. of parameters for αL-H$_2$O	15
No. of background points refined	32
No. of bond length restraints	24
No. of bond angle restraints	35
R_p	0.0657
R_{wp}	0.0733
R_{exp}	0.0222
χ^2	10.9
R_B	0.0163
R_F	0.0223

Table 3
Profile and structural parameters for the hygroscopic and monohydrate phases of α-lactose obtained with *FullProf* after Rietveld refinements.

	αL$_H$	αL-H$_2$O
U_{ST}	–	0.038 (8)
Y_{SZ}	0.057 (2)	0.044 (4)
G_{SZ}	−0.0016 (3)	–
S_{400}	0.438 (47)	–
S_{040}	0.0119 (6)	–
S_{004}	11.26 (31)	–
S_{220}	−0.012 (13)	–
S_{202}	7.92 (50)	–
S_{022}	0.17 (6)	–
S_{121}	−0.06 (7)	–
S_{301}	−0.68 (24)	–
S_{103}	9.02 (64)	–
Asym$_1$	0.018 (7)	0.018 (7)
Asym$_2$	0.015 (1)	0.015 (1)
Preferred orientations	[0, 0, 1]	[0, 1, 0]
G_1	1.089 (4)	1.011 (6)
B_{iso} (Å^2)	2.81 (13)	2.01 (32)
Proportion (%)	83 (1)	17 (1)

Table 4
Torsion angles (°) of the β-1,4 linkage in several disaccharides.

ψ_1, ψ_1', ψ_2 and ψ_2' are defined by Sundaralingam (1968).

	αL$_H$†	αL-H$_2$O‡	βL§	βC¶	m-βC††
ψ_1 O5—C1—O1—C4$'$	−92.3 (11)	−92.6	−70.7	−76.3	−91.1
ψ_1' C2—C1—O1—C4$'$	148.1 (9)	146.2	170.3	166.5	152.1
ψ_2 C1—O1—C4$'$—C3$'$	91.5 (11)	94.6	108.0	106.4	80.3
ψ_2' C1—O1—C4$'$—C5$'$	−150.9 (9)	−143.0	−131.3	−132.3	−160.7

† This paper. ‡ Fries *et al.* (1971). § Hirotsu & Shimada (1974). ¶ β-Cellobiose (Chu & Jeffrey, 1968). †† Methyl β-cellobioside (Ham & Williams, 1970).

3. Discussion

The mean values of the bond lengths are 1.528 (9) Å for C_{int}—C_{int}, 1.434 (12) Å for C_{int}—O_{int} and 1.420 (9) Å for C_{int}—O_{per}, C_{int}—O_{link} and C_m—O_m. These values are close to the mean values obtained in other disaccharides with a β-1,4 linkage (see Table 1). The maximum deviation from these mean values (0.020 Å) occurs for the C2—O2 bond. For the β-1,4 linkage, the C1—O1 and C4$'$—O1 bonds lengths are similar (1.427 and 1.432 Å, respectively), while the difference between these two bond lengths is of the order of 0.05 Å in other disaccharides [see, for example, Table 5 of Hirotsu & Shimada (1974)]. For the bond angles, the mean values are 109 (3)° for C_{int}—C_{int}—C_{int}, 118 (4)° for C_{int}—C_{int}—O_{int}, 106.3 (3)° for C_{int}—O_{int}—C_{int} and 111 (4)° for C_{int}—C_{int}—O_{per}. The mean values of the angles involving O_{int} atoms differ from those found in other disaccharides: by about 7° for C_{int}—C_{int}—O_{int} and 6° for C_{int}—O_{int}—C_{int}. The value of the linkage angle C1—O1—C4$'$ is 111.5 (5)°, that is, 5° smaller than in other disaccharides [see Table 6 of Hirotsu & Shimada (1974)]. Table 4 reports the torsion angle values of the β-1,4 linkage for some disaccharides. The two forms of α-lactose exhibit a symmetrical twist about the bridging bond, with very similar torsion angles: ψ_1 = −92.3 and ψ_2 = 91.1° for αL$_H$, and ψ_1 = −92.6 and ψ_2 = 94.6° for αL-H$_2$O (Fries *et al.*, 1971). In contrast to the α-lactose structures, an asymmetric twist about the bridging bond is found in βL (Hirotsu & Shimada, 1974) and β-cellobiose (Chu & Jeffrey, 1968), with a difference $|\psi_2| - |\psi_1|$ of the order of 34°. Methyl β-cellobioside (Ham & Williams, 1970) has an intermediate conformation, with a $|\psi_2| - |\psi_1|$ value of *ca* 11°.

As for other disaccharides with a β-1,4 linkage, the O3$'$—HO3$'\cdots$O5 intramolecular hydrogen bond exists in αL$_H$ and plays a fundamental role in the molecular conformation.

In both αL-H$_2$O and αL$_H$, the molecules are oriented with their long axis parallel to the twofold screw axis. As a consequence, the two forms have the same space group, $P2_1$, and their lattice parameters are similar: a = 7.7795, b = 19.693, c = 4.9064 Å and β = 103.69° for αL$_H$, and a = 7.9423, b = 21.599, c = 4.8168 Å and β = 109.75° for αL-H$_2$O, obtained with a Rietveld refinement from the commercial powder used to obtain the αL$_H$ phase by annealing. The loss of the water molecule leads to a significant decrease of the b parameter only. The ratio between the two unit-cell volumes ($V_{\alpha LH}/V_{\alpha L-H_2O}$ = 0.939) is close to the ratio of the number of atoms in the cells (45/48 = 0.938).

For carbohydrates, the cohesion lattice energy is mostly provided by O—H$\cdots$O hydrogen bonds, and for this discussion, it is interesting to compare the hydrogen-bonding networks of the two forms of α-lactose (αL$_H$ and αL-H$_2$O) and to try to draw some conclusions about the instability of the αL$_H$ form. The hydrogen-bonding distances and angles for the αL$_H$ form are listed in Table 5. Fig. 3 gives an *ORTEP* plot (Farrugia, 1997) of the projection of the cell along c^*, and Fig. 4 shows the projection of the cell along the twofold axis, with only the molecules around $y = 0$. In these plots, the hydrogen

Table 5
Hydrogen-bonding geometry (Å, °) for the hygroscopic phase of α-lactose.

| $D-H\cdots A$	$D-H$	$H\cdots A$	$D\cdots A$	$D-H\cdots A$
O2$-$HO2$\cdots$O6^i	1.009 (19)	1.883 (21)	2.854 (21)	160.8 (13)
O3$-$HO3$\cdots$O5$'^{ii}$	0.989 (20)	2.078 (16)	2.809 (16)	129.2 (13)
O4$-$HO4$\cdots$O2$'^{iii}$	0.998 (21)	1.924 (19)	2.849 (19)	152.8 (15)
O6$-$HO6$\cdots$O2^{iv}	1.002 (17)	1.789 (18)	2.767 (18)	164.2 (15)
O1$'-$HO1$'\cdots$O3^v	0.999 (20)	1.810 (20)	2.736 (20)	152.7 (15)
O2$'-$HO2$'\cdots$O6$'^{iv}$	1.054 (19)	1.953 (16)	2.800 (18)	135.0 (13)
O3$'-$HO3$'\cdots$O5	1.000 (21)	1.873 (17)	2.697 (18)	137.6 (15)
O6$'-$HO6$'\cdots$O3$'^i$	1.016 (21)	1.803 (17)	2.674 (19)	141.5 (15)

Symmetry codes: (i) $x+1, y, z$; (ii) $-x+1, y+\frac{1}{2}, -z+2$; (iii) $-x, y+\frac{1}{2}, -z+1$; (iv) $x-1, y, z-1$; (v) $-x+1, y-\frac{1}{2}, -z+1$; (vi) $x, y, z-1$; (vii) $-x+1, y-\frac{1}{2}, -z+2$; (viii) $x, y, z+1$; (ix) $x-1, y, z$.

bonds are drawn as dashed lines. The O atoms of the eight hydroxy groups of the molecule are all donors; atoms O2, O3, O5 and O6 of the galactose unit are acceptors, and for the glucose unit, the acceptor atoms are O2$'$, O3$'$, O5$'$ and O6$'$. As reported for αL-H$_2$O, atoms O1, O4 and O1$'$ in αL$_H$, the central and furthest O atoms of the rings, are not acceptors. The O$\cdots$O distances range from 2.674 (19) to 2.854 (21) Å, with a mean value of 2.77 (7) Å. The H$\cdots$O bond lengths range from 1.789 (18) to 2.078 (16) Å, with a mean of 1.89 (10) Å. These distances are in agreement with those generally found in carbohydrates (Jeffrey, 1990). The O$-$H$\cdots$O bond angles range from 129.2 (13) to 164.2 (15)°; the maximum value given by Jeffrey (1990) for this angle is $\sim$160°.

Both forms contain an infinite chain of hydrogen bonds; the successive hydrogen bonds are as follows[3] (symmetry codes are given at the bottom of Table 5)

$$\to O2 \to O6^i \to O2^{vi} \to .$$
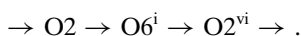
The molecule at the origin of this chain is first connected to its neighbour along a; then, the last molecule is linked to the molecule at $(x, y, z-1)$. These chains of hydrogen bonds lie along the c axis, but there are strong interactions between neighbouring molecules located in the same monoclinic ac plane. The two forms also have a common finite chain
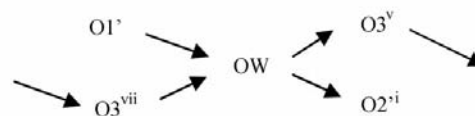
$$O4^{vii} \to O2'^{viii} \to O6'^{ix} \to O3' \to O5.$$
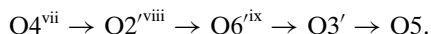
This chain includes the intramolecular O3$'-$HO3$'\cdots$O5 hydrogen bond. Among the other hydrogen bonds, two of them involve molecules in the same monoclinic plane, and only the O4$-$HO4$\cdots$O2$'$ bond connects molecules along the twofold screw axis. The chains containing the remaining hydrogen bonds are different for the two forms. For αL$_H$, there is a small finite chain

$$O1' \to O3^v \to O5'^{vi}.$$
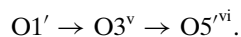
However, in the case of αL-H$_2$O, the remaining H atoms of the hydroxy groups are connected to the water molecule, and

---

[3] In order to make comparisons between the two forms, reduced coordinates of the αL-H$_2$O form obtained by Fries *et al.* (1971) were translated by $(0, -y_{O1}, \frac{1}{2})$ for the α-lactose molecule and $(0, -y_{O1}, -\frac{1}{2})$ for the water molecule ($y_{O1} = 0.2944$).

the H atoms of the water molecule also form new hydrogen bonds

with an O3 $\to$ OW $\to$ O3 infinite chain. The O2$'$ atom is twice an acceptor and the OW $\to$ O2$'$ hydrogen bond connects this infinite chain to the finite chain O4$^{vii} \to$ O2$'^{viii} \to$ O6$'^{ix} \to$ O3$' \to$ O5. The interconnections between hydrogen-bonding
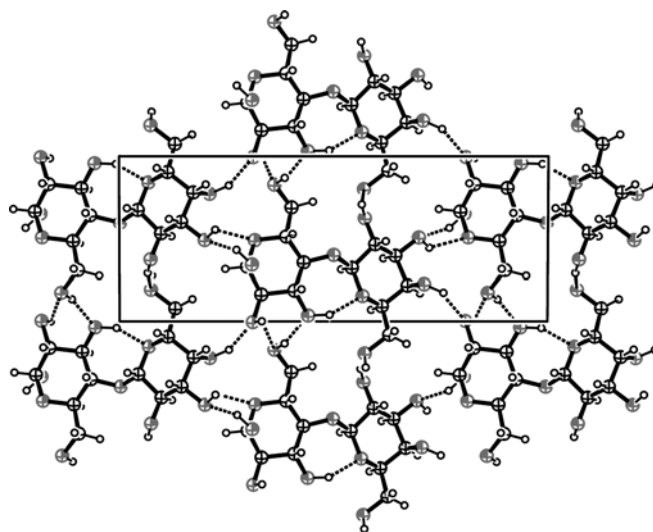

Figure 3
Projection of the unit cell of the hygroscopic α-lactose along c^*. Dashed lines correspond to hydrogen bonds.
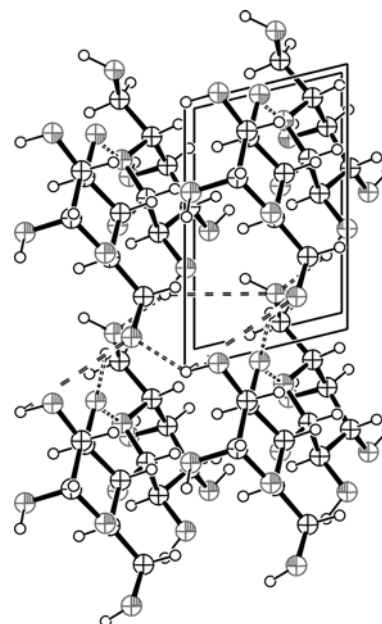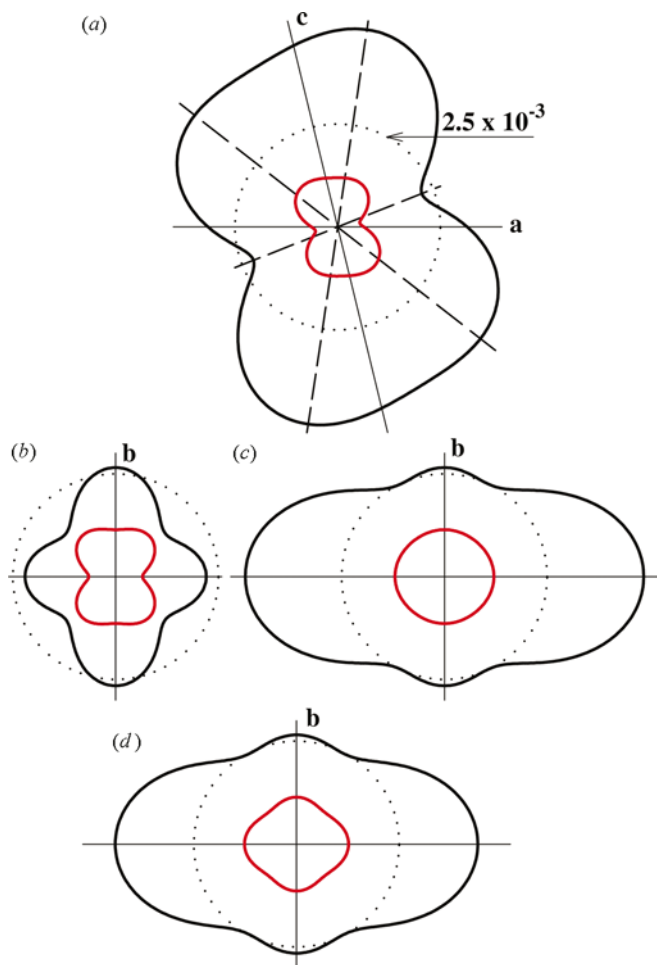

Figure 4
Projection of the unit cell of the hygroscopic α-lactose along the twofold screw axis. Only molecules around $y = 0$ are drawn. Dashed lines correspond to hydrogen bonds.

Preliminary Rietveld refinements for the commercial αL-H_2O powder lead to an average diameter of 1400 Å for the crystallites and an average strain of the cell of 11.1×10^{-4}. After annealing at 408 K, the corresponding values become 730 Å and 9.0×10^{-4} for the αL-H_2O phase, and 790 Å and 31.2×10^{-4} for the αL$_H$ phase. The size of the crystallites is almost identical for the two phases and is about one-half of the size of the starting compound, the size reduction being due to breakage of the crystallites when the powder is heated. The strain effects are, generally, due to defects in the lattice (vacancies, impurities *etc.*), and in a lattice such as αL$_H$, possible defects are the breaking of a hydrogen bond or the presence of a residual water molecule. The average values of these strain effects are similar in the αL-H_2O phase before and after annealing. For αL$_H$, the average value is three times greater than that of αL-H_2O. In fact, these strain effects have a strong anisotropic character, and Fig. 5 shows the value of this strain for different planes of the lattice. The value of the strain ranges from 17.2×10^{-4} for the 120 reflection to 48.4×10^{-4} for 103. In the monoclinic plane, the minimum value of the strain (22.0×10^{-4}) occurs for $\varphi = 21.5°$, and the strain has a value higher than 43.0×10^{-4} for a large area around the c axis ($\varphi = 60$–$155°$). As seen above, the cohesion energy in the monoclinic plane is provided by hydrogen bonds. From Fig. 4, it can be concluded that no hydrogen bond exists in the monoclinic plane for $\varphi \simeq 21°$. Conversely, there are several hydrogen bonds around the direction of the lattice parameter c, and the high value of the strain can indicate a breaking of chains of the hydrogen-bonding networks. Along the twofold axis, the strain has an intermediate value (26.5×10^{-4}) corresponding to the absence of residual water molecules and an almost complete formation of the hydrogen bonds characteristic of the αL$_H$ phase.

To conclude, the structure determination of the hygroscopic phase of α-lactose is consistent with two possible reasons for the instability of this phase: the destruction of the hydrogen-bonding networks along the twofold axis when the water molecule is removed and the existence of many defects in the hydrogen-bonded chains.

Figure 5
Strain values on the αL$_H$ phase for different directions of the lattice (black curves) (*a*) in the monoclinic plane, and (*b*), (*c*) and (*d*) in planes formed by the twofold axis and a direction of an extreme value of the strain in the monoclinic plane (φ is the angle between the lattice parameter *a* and this direction). (*b*) $\varphi = 21.5°$, (*c*) $\varphi = 81°$ and (*d*) $\varphi = 142°$. The red curves correspond to the strain values for commercial αL-H_2O.

chains, absent from the αL$_H$ form, must be an important factor for the stability of the αL-H_2O form. In this form, atoms O1 and O3^v are 4.662 (12) Å apart and are connected *via* the OW atom. In the αL$_H$ phase, with the loss of the water molecule, the two atoms move closer and form a hydrogen bond with an O1$'\cdots$O3^v distance of 2.736 (20) Å.

An original aspect given by the powder diffraction pattern is the possibility of deducing from the shape and the width of the Bragg peaks the average size of the crystallites and the strain of the cell. In the present case, for the αL$_H$ phase, the size effects are considered as isotropic and the strain effects as anisotropic, and for the αL-H_2O phase, the two effects are taken as isotropic. Isotropic size effects (spherical shape of the crystallites) for the two phases are consistent with the calculated effects of the preferred orientations; for αL$_H$, $G_1 = 1.089$ (4) for the [001] preferred direction, corresponding to a weak platy habit of the crystallites. For the αL-H_2O phase, where $G_1 = 1.011$ (6), there is, in practice, no preferred orientation.

References

Beevers, C. A. & Hansen, H. N. (1971). *Acta Cryst.* B**27**, 1323–1325.
Bérar, J. F. & Baldinozzi, G. (1993). *J. Appl. Cryst.* **26**, 128–129.
Brückner, S. & Immirzi, A. (1997). *J. Appl. Cryst.* **30**, 207–208.
Buma, T. J. & Wiegers, G. A. (1967). *Neth. Milk Dairy J.* **21**, 208–213.
Caglioti, G., Paoletti, A. & Ricci, F. P. (1958). *Nucl. Instrum.* **3**, 223–228.
Chu, S. & Jeffrey, G. A. (1968). *Acta Cryst.* B**24**, 830–838.
Dollase, W. A. (1986). *J. Appl. Cryst.* **19**, 267–272.
Evain, M., Deniard, P., Jouanneaux, A. & Brec, R. (1993). *J. Appl. Cryst.* **26**, 563–569.
Farrugia, L. (1997). *J. Appl. Cryst.* **30**, 565.
Favre-Nicolin, V. & Cerny, R. (2002). *J. Appl. Cryst.* **35**, 734–743.
Fries, D. C., Rao, S. T. & Sundaralingam, M. (1971). *Acta Cryst.* B**27**, 994–1005.
Garnier, S. (2001). Thesis, University of Rouen, France.

Ha, S. N., Giammona, A., Field, M. & Brady, J. W. (1988). *Carbohydr. Res.* **180**, 207–221.

Ham, J. T. & Williams, D. G. (1970). *Acta Cryst.* B**26**, 1373–1383.

Hirotsu, K. & Shimada, A. (1974). *Bull. Chem. Soc. Jpn*, **47**, 1872–1879.

Jeffrey, G. A. (1990). *Acta Cryst.* B**46**, 89–103.

Kreveld, A. van (1969). *Neth. Milk Dairy J.* **23**, 258–275.

Le Bail, A., Duroy, H. & Fourquet, J. L. (1988). *Mater. Res. Bull.* **23**, 447–452.

March, A (1932). *Z. Kristallogr.* **81**, 285–297.

Noordik, J. H., Beurskens, P. T., Bennema, P., Visser, R. A. & Gould, R. O. (1984). *Z. Kristallogr.* **168**, 59–65.

Rodriguez-Carvajal, J. (2001). *FullProf.* Version 1.9c. LLB, CEA/Saclay, France.

Rodriguez-Carvajal, J. & Roisnel, T. (2004). *Proceedings of EPDIC* 8, edited by Y. Andersson, E. J. Mittemeijer & U. Welzel, pp. 123–126. Zürich: Trans Tech Publications.

Roisnel, T. & Rodriguez-Carvajal, J. (2002). *Mater. Sci. Forum*, **378–381**, 118–123.

Sundaralingam, M. (1968). *Biopolymers*, **6**, 189–213.

Smith, G. S. & Snyder, R. L. (1979). *J. Appl. Cryst.* **12**, 60–65.

Smith, W. & Forester, T. R. (1996). *J. Mol. Graphics*, **14**, 136–141.

Stephens, P. W. (1999). *J. Appl. Cryst.* **32**, 281–289.

Thompson, P., Cox, D. E. & Hastings, J. B. (1987). *J. Appl. Cryst.* **20**, 79–83.

Werner, P. E., Eriksson, L. & Westdahl, M. (1985). *J. Appl. Cryst.* **18**, 367–370.

Wolff, P. M. de (1968). *J. Appl. Cryst.* **1**, 108–113.